Copy 5
RM L52H20

NACA

RESEARCH MEMORANDUM

A TRANSONIC INVESTIGATION OF THE AERODYNAMIC CHARACTERISTICS OF PLATE- AND BELL-TYPE OUTLETS FOR AUXILIARY AIR

By William J. Nelson and Paul E. Dewey

Langley Aeronautical Laboratory
Langley Field, Va.

NATIONAL ADVISORY COMMITTEE
FOR AERONAUTICS

WASHINGTON
September 3, 1952

NATIONAL ADVISORY COMMITTEE FOR AERONAUTICS

RESEARCH MEMORANDUM

A TRANSONIC INVESTIGATION OF THE AERODYNAMIC CHARACTERISTICS OF PLATE- AND BELL-TYPE OUTLETS FOR AUXILIARY AIR

By William J. Nelson and Paul E. Dewey

SUMMARY

Aerodynamic characteristics of several plate- and bell-type outlets discharging air into a transonic stream have been investigated. The data presented herein show the variation in the discharge coefficient of such outlets as a function of the rate of discharge. The discharge rate is expressed nondimensionally in terms of the rate at which air from the undisturbed stream would flow through a tube whose cross section was equal to the area of the outlet. For outlets of the types tested, discharge characteristics obtained at low speeds can probably be applied at transonic Mach numbers if the free-jet characteristics of the outlet are first corrected for the effects of Reynolds number and pressure ratio. Total-pressure surveys through the jet wake are compared at Mach numbers of 0.7, 1.1, and 1.3 for the different outlets investigated. Static-pressure distribution in the vicinity of circular outlets is shown for several Mach numbers and discharge rates.

INTRODUCTION

The increased demand for auxiliary air which has accompanied cabin pressurization and the development of jet-powered transonic aircraft has emphasized the need for experimental data on the high-speed, aerodynamic characteristics of small outlets. Although the performance of an airplane may not be seriously impaired by inefficient design of a single outlet discharging a relatively small quantity of air, it is apparent that the cumulative effect of many such openings scattered over the airplane discharging a volume of air equal to some 5 to 8 percent of that required by the engines might impose significant penalties in over-all performance. A substantial volume of data on outlet design is available from tests at Mach numbers below 0.35. The applicability of these data to the transonic airplane has not been established. It is the purpose of this report to

make available to the designers of high-speed airplanes some preliminary outlet-design data obtained in recent tests at transonic Mach numbers.

Several outlets of circular and elliptical cross section have been installed in a flat plate and tested in a uniform stream at Mach numbers from 0.7 to 1.3. The effects of several geometric parameters (outlet diameter, cross section, and the presence of a faired, bellmouthed approach section ahead of the opening) on the discharge coefficient and extent of flow disturbances resulting from varying rates of discharge are presented. To facilitate comparison with available low-speed data, the direction of discharge was normal to the main flow direction. For these tests the pressure gradient over the surface was zero with no flow from the outlet, the stagnation temperature of the discharge air was the same as that of the main stream, and the stagnation pressure of the discharge flow was equal to or less than that of the free stream. These results are part of a continuing study of outlet characteristics in progress in the Internal Aerodynamics Section of the Langley Aeronautical Laboratory.

SYMBOLS

A	cross-sectional area of outlet
D	outlet diameter
K	outlet discharge coefficient (general), $\frac{\text{Actual mass flow}}{\text{Theoretical mass flow}}$
K_o	outlet discharge coefficient as free jet, $\frac{\text{Actual mass flow}}{\text{Theoretical mass flow}}$
M	Mach number
m	mass flow through outlet
P	local stagnation pressure
P_o	stagnation pressure in free stream
p	local static pressure
R	Reynolds number
V	velocity in free stream

[redacted]

x	streamwise distance from center line of outlet
y	distance normal to outlet surface
z	distance transverse to stream measured from center line of outlet
ρ	mass density
δ	boundary-layer thickness

APPARATUS

Figure 1 shows the tunnel used in this investigation with one side plate removed and a cutaway outlet model mounted in the upper floor. The test section was $4\frac{1}{2}$ inches high, $6\frac{1}{4}$ inches wide, and 17 inches long. The upper floor was a solid flat plate with a circular opening in which the various outlet models were mounted. The lower floor was slotted with one-fifth of the area open. The chamber surrounding the tunnel test section was kept at pressures well below atmosphere by means of the laboratory vacuum pump which permitted controlled removal of air from the test section and the generation of supersonic Mach numbers up to 1.3.

The general arrangement of setup used is shown schematically in figure 2. The air discharged through the outlet was taken from the tunnel supply duct and supplied to the outlet through a 2-inch pipe. The discharge rate was controlled by a valve and measured with a calibrated orifice meter located in the outlet air line. The flow rate was calculated from pressures read at pipe taps upstream and downstream of the metering orifice. In order to determine the outlet discharge coefficient, a pipe tap was located in the outlet air line, and the static pressure of the undisturbed stream in the tunnel was taken as the discharge pressure. Fine-mesh screens were installed in the outlet air line upstream of the metering orifice and outlet to insure a uniform velocity distribution.

Two types of outlets discharging perpendicular to the tunnel floor were used, figure 3. The three thin-plate, $\frac{1}{16}$-inch-thick, outlets of circular cross section 3/8 to 7/8 inch in diameter and an elliptical outlet with a major to minor axis ratio of 2 to 1 were machined from brass. The three bellmouthed outlets varying in diameter from 1/4 to 7/8 inch were cast in plastic.

Instrumentation with the various setups included orifices located in the upper floor of the tunnel along the center line. The location of these orifices is indicated in the cutaway model shown in figures 1 and 3. Total-pressure surveys were made in the wake of the outlet with a rake of 11 total-pressure tubes. These surveys were made in a plane perpendicular to the axis of the tunnel and 1 inch downstream from the center line of the outlet.

Surface pressures and total pressures were indicated on a mercury manometer and recorded photographically. At the same time, the pressures used to calculate outlet discharge rate and discharge coefficient were read visually.

RESULTS

Prior tests in transonic test sections of the same type as that used in this investigation indicate that tunnel-wall interference effects may be neglected for the purposes of this investigation.

Discharge coefficient.- In conducting these tests, the free-stream Mach number was fixed at predetermined values between 0.7 and 1.3 and the rate of discharge was varied by adjustment of the outlet control valve shown in figure 2. The resulting change in outlet velocity relative to that of the free stream is accompanied by simultaneous variations in jet Reynolds number and jet Mach number. To separate the effect of these various parameters on the discharge coefficient, a free-jet calibration of each outlet was made over a range of jet Reynolds numbers from 5,000 to 600,000 and jet pressure ratios up to 3.0. The Reynolds number is based on outlet diameter and the theoretical flow rate. The free-jet discharge coefficient, defined as the ratio of the measured rate of discharge to the theoretical rate corresponding to the measured pressure difference across the outlet, is shown in figure 4 for plate-type outlets of circular and elliptical cross section. At free-jet pressure ratios greater than 1.89, the outlet is considered choked; thus the theoretical flow rate becomes independent of the pressure ratio P/p but varies directly with P. Data at Reynolds numbers above 80,000 were taken from reference 1; data at lower Reynolds numbers, from the present tests.

At $M < 0.7$ ($P/p < 0.7$) the discharge coefficient of the circular outlets increased rapidly with Reynolds number to $RN \approx 10^4$. At Reynolds numbers above 10^4 and Mach number greater than 0.6, lines of constant discharge coefficient are nearly vertical; in this range the effect of jet Reynolds number is small and the Mach number effect is

[redacted]

large. Transition between predominance of the Reynolds number and Mach number effects occurs smoothly at discharge coefficients on the order of 0.68. These results are consistent with well-established effects of Reynolds number and Mach number on the jet diameter at the vena contracta. The discharge coefficients for outlets of elliptical cross section, figure 4(b), are generally similar to those observed for circular outlets, figure 4(a).

With the bellmouthed outlets the discharge coefficient was increased to values approaching unity, 0.93 to 0.95 at $M < 0.6$; at pressure ratios greater than 1.89 and Reynolds numbers greater than 30,000, K_o reached a value of 0.97. Because of the small variation, these data are not presented.

Results of tests in which air was discharged from plate and bellmouthed outlets into a uniform stream are presented in figure 5. The discharge coefficient plotted in this figure is based on a theoretical flow rate which assumes an outlet static pressure equal to the free-stream static. The nondimensional parameter $m/\rho VA$ is used to define the discharge rate; it is the ratio of the measured discharge rate to the rate at which free-stream air would flow through an area equal to that of the outlet.

For plate-type outlets of circular cross section, these curves, which over the range of the current tests are essentially independent of stream Mach number, have a maximum slope at $\frac{m}{\rho VA} = 0$ where K also is zero, figure 5(a). Each curve appears to approach a maximum coefficient at $\frac{m}{\rho VA} \approx 0.8$. As previously mentioned, increases in jet Reynolds number and jet pressure ratio accompany increases in $m/\rho VA$ along each curve. The displacement of curves from tests of outlets of different diameter is in part the result of changes in Reynolds number; however, it is also influenced by decrease in the relative thickness of the surface boundary layer as the outlet diameter increases; that is, δ/D decreases. Separation of boundary-layer effect and the effect of mass flow ratio $m/\rho VA$ from the Reynolds number and Mach number effects will be discussed later. It is sufficient at this point, however, to note that, at mass flow ratios below unity, the combined effects of all other variables are relatively small.

For thin-plate outlets of elliptical cross section, the value of K increases with $m/\rho VA$ as shown in figure 5(b). The curves for the circular outlet of approximately the same area follow the lower curve (major axis transverse to undisturbed flow) very closely, within ±0.02. Alinement of the major axis of the elliptical outlet with the stream is shown to result in substantially higher discharge coefficients at corresponding values of the mass flow parameter. The difference between the value of

[redacted]

K for outlets thus alined and for those turned 90° to this direction decreases rapidly as the free-stream Mach number increases.

For bellmouthed outlets, figure 5(c), the discharge coefficient increases with mass flow parameter reaching values somewhat greater than those measured with plate-type outlets. Slightly higher maximum coefficients were measured with the larger outlets. The effect of Mach number was small.

To isolate the influence of flow ratio variations on the discharge coefficient, the data of figures 5(a) to 5(c) are replotted in figures 6(a) to 6(c) with the coefficient expressed in terms of the free-jet coefficient at identical values of the jet Reynolds number and pressure ratio. Plotted in this manner the curves for plate-type outlets are observed to reach definite maxima at values of K appreciably greater than the corresponding free-jet coefficients. The occurrence of discharge coefficients in excess of the free-jet coefficients is probably a result of localized disturbances in the flow near the outlet which effect a reduction in static pressure at the outlet. To facilitate direct application of these data, the static pressure in the undisturbed stream has been used throughout this report in calculations of theoretical mass flows. The occurrence of a maximum value of the ratio K/K_o was also observed by Rogallo in the data taken at stream Mach numbers of 0.05 and 0.11, reference 1. These results are superimposed on the data for $M = 0.7$ of figure 6(a). It is apparent from these data that for thin-plate outlets of circular cross section, the results of low-speed tests may be applied in the transonic range with a maximum error on the order of 10 percent.

Similar data from reference 2 at a free-stream Mach number of 0.35 are also presented in figure 6(a). The displacement between these data and those of reference 1 and the current program at $\frac{m}{\rho VA} \approx 1.0$ is probably caused by the difference in temperature between the jet and main stream; that is, $T_{o_j} - T_o \approx 300$ in reference 2 and 0° in reference 1 and the current program.

Although a single curve is drawn through the experimental data for all three outlets tested, a tendency toward higher coefficients with small outlets is observed which is probably associated with the increase in boundary-layer thickness relative to the outlet diameter δ/D. Since the boundary layer in all these tests was very small, the effect of changes in δ is also small. For very thick boundary layers, the effective stream velocity at the point of exit is decreased thereby increasing the effective value of $m/\rho VA$. It is apparent that, if the small outlets are to be installed in regions of very thick boundary layers, a correction must be applied to the stream velocity which appears in the $m/\rho VA$ parameter.

[redacted]

At a free stream Mach number of 0.7, discharge coefficients with elliptical outlets with the major axis parallel to the direction of flow were more than 30 percent greater than the free-jet coefficients, and 15 percent greater with the major axis turned 90° to the free stream. Corresponding gain with circular outlets approached 20 percent. The effects of outlet alinement and shape decrease with increasing stream Mach number until at $M = 1.3$ the over-all spread in the K/K_o curves is on the order of 5 percent.

With the addition of the bellmouthed approach section in the circular outlets, the slope of the K/K_o against $m/\rho VA$ curve decreased substantially. Compare figures 6(c) and 6(a). The value of K/K_o increases continuously approaching a value of unity at mass flow ratios, $\frac{m}{\rho VA} \approx 0.8$; it appears probable that values in excess of unity would be reached at flow rates greater than those investigated herein.

Jet wake.- Typical results of total-pressure surveys in a plane 1 inch downstream from the center of the $\frac{5}{8}$- inch plate-type outlet $\left(\frac{x}{D} = 1.6\right)$ are presented in figure 7 as contours of constant pressure. Along the outer contour the measured total pressure was equal 0.9 of that in the undisturbed stream, 0.8 along the second contour, etc. At all Mach numbers, the minimum total pressure measured in the center of the wake approximated the value of the static pressure in the undisturbed stream. The influence of the jet at $\frac{x}{D} = 1.6$ is confined to a region extending approximately 1 to 1.5 jet diameters to each side of the plane of symmetry. Outside of this region, contours of constant total pressure are essentially parallel to the wall corresponding to uniform boundary layer across the tunnel wall. Something of the nature of the flow in the vicinity of the jet may be deduced from an examination of the shape of the total-pressure contours. At low flow rates the boundary layer appears to have been displaced upward by the jet; as the flow rate increases, however, contours near the edge of the jet are displaced downward until at the highest values of $m/\rho VA$, the boundary layer at the edge of the wake disappears. This reduction in thickness of the boundary layer at the edges of the jet wake is brought about by vortices which, set up by the action of the jet, carry high energy air from the undisturbed stream toward the wall. The action of these vortices which increase in strength with $m/\rho VA$ also accounts in part for an observed widening of the upper part of the wake with increasing $m/\rho VA$. The existence of strong vortices at the edges of the jet renders measurement of total pressure both difficult and inaccurate in these regions. The contours of figure 7 must therefore be regarded as qualitative. Similar data from tests of elliptical and bellmouthed outlets follow the same general pattern observed in figure 7.

[redacted]

The errors caused by misalinement of survey tubes with direction of flow are probably smaller in the plane of symmetry than at the edge of the jet; consequently, these data are presented in greater detail. The stagnation pressure directly behind the outlet expressed in terms of free-stream stagnation pressure is presented in figures 8(a) to 8(c) as a function of vertical distance from the wall. Constancy of the pressure gradient through the outer part of the wake again suggests that the jet action has been to locally push the boundary layer out into the stream, the absolute displacement increasing almost linearly with rate of flow from the opening. The development of reversals in the pressure gradient in the inner part of the wake, close to the wall, is attributed to the vortex action previously discussed. An outward displacement of the center of the vortex with increasing rate of discharge is also evident from these curves. Increasing free-stream Mach number resulted in increased magnitude of the pressure differential through the wake and a small reduction in the effect of mass flow ratio.

Because all surveys were carried out at a constant distance of 1 inch from the center line of the outlet, a change in outlet diameter results in a change in location of the survey plane relative to the diameter of the hole; thus with a $\frac{7}{8}$-inch outlet the survey plane is 1.14 diameters downstream, and 2.67 diameters with the $\frac{3}{8}$-inch outlet. With increasing distance x/D downstream, little change is found in the general characteristics of the wake although some differences in the absolute value of the pressure and the gradient are observed.

Similar curves for plate-type outlets of elliptical cross section are presented in figure 8(b). These show a very strong effect of axis alinement relative to the direction of flow in the main stream. With the major axis of the outlet transverse to the free stream, the total-pressure gradient through the outer part of the wake is very steep and the jet penetration is observed to be smaller than that observed at the same flow rate and Mach number from outlets of circular cross section or elliptical outlets whose major axis was parallel to the flow. With the major axis parallel to the stream, the pressures in the center of the wake are appreciably higher than those for other configurations. Explanation for this is again found in the vortices which, with major axis parallel to the stream, are close together and somewhat stronger as a result of the greater area of contact between sides of jet and the main stream. Thus the stronger tendency of the jet to separate into two vortices with the losses concentrated at the center of each results in higher pressures in the plane of symmetry.

In the wake of bellmouthed outlets the total pressure, figure 8(c), follows the same pattern observed behind the plate-type openings of

circular cross section. At $M = 0.7$ the results are somewhat more erratic than at higher Mach numbers where the pressure gradient through the edge of the wake is essentially the same for plate and bell-type outlets and the distance which the jet penetrates into the stream decreases with the addition of a smooth approach to the outlet.

The vortex effect observed at the higher flow rates may be of considerable significance if the gases being discharged were at high temperature, for it appears probable that dilution of the exhausted gases with cooler, high-energy air from the adjacent stream would effect substantial reductions in temperature of the gas along the wall. It is pointed out, however, that the effectiveness of such cooling is dependent upon the value of $m/\rho VA$. This tendency of the jet to be lifted off the surface at high flow rates may also make possible the discharging of toxic or otherwise objectionable gases without danger of their being returned to the airplane through auxiliary inlets located further downstream.

Surface pressure distribution.- The variation of surface pressure along a line through the center of $\frac{3}{8}$-inch circular outlets is shown in figure 9. The distance, in outlet diameters, is measured from the center of the outlet. The local static pressure is presented as a nondimensional parameter $\Delta p/q$ where Δp is the difference between the surface pressure and the static pressure of the undisturbed stream, and q is the dynamic pressure of the undisturbed stream. Experimental data from the zero flow tests are shown on each figure, curves for $m/\rho VA$ of 0.2, 0.4, and 0.6 were obtained by interpolation. Approaching the outlet from upstream, the surface pressure increases over a region extending several diameters ahead of the outlet probably approaching the full stagnation pressure over the outlet. The rate of rise and the extent of the region influenced by the outlet flow increase with rate of discharge. Immediately downstream of the outlet, surface pressures far below the stream pressures were encountered; these pressures result from curvature of the stream lines as they close around the jet. Further downstream, the pressure returns rapidly to the undisturbed stream static. At supersonic free-stream Mach numbers, the pressure rise on the upstream side is much more abrupt than at $M < 1.0$; the position of the detached bow shock caused by the outlet discharge is well-defined moving closer to the outlet as the stream Mach number increases.

The addition of a straight approach section ahead of the outlet causes no significant change in pressure distribution in the vicinity of the outlet, figure 9(b). Lower pressures at corresponding points behind the bellmouthed outlets indicate that the stream, close to the surface, suffers less deviation in flowing around the jet from the thin plate than it does in flowing around the more cylindrical jet from the bellmouth.

[redacted]

CONCLUSIONS

From this investigation of the transonic aerodynamic characteristics of small outlets of thin-plate and bellmouthed designs, it is concluded that:

1. For these types of outlets, the flow discharge characteristics obtained from tests in free stream at low Mach number can probably be applied with satisfactory accuracy at transonic free-stream Mach numbers when corrected for pressure ratio and Reynolds number effects on the characteristics of the free jet.

2. The discharge coefficient of plate-type outlets increases with rate of discharge from zero to a maximum value in excess of the free-jet coefficient decreasing thereafter to the free-jet value. At a constant value of the mass flow parameter $m/\rho VA$ the discharge coefficient decreases slightly with increasing stream Mach number.

3. Discharge coefficients for thin-plate outlets of elliptical cross section are increased by alining the major axis of the ellipse to the direction of flow in the undisturbed stream.

4. Discharge coefficients of circular outlets are increased substantially at the higher flow rates by the addition of a bellmouthed approach section ahead of the opening.

5. A jet discharged from a smooth surface over which air is flowing induces vortices which bring high-energy air from the free stream under the jet and thus tend to lift the discharged gas from the surface.

6. The static pressure immediately ahead of the outlet increased substantially and behind the outlet decreased to values well below the static pressure of the free stream. The amount of the change increases with rate of discharge from the outlet.

Langley Aeronautical Laboratory,
National Advisory Committee for Aeronautics,
Langley Field, Va.

[redacted]

REFERENCES

1. Rogallo, F. M.: Internal-Flow Systems for Aircraft. NACA Rep. 713, 1941.

2. Callaghan, Edmund E., and Bowden, Dean T.: Investigation of Flow Coefficient of Circular, Square, and Elliptical Orifices at High Pressure Ratios. NACA TN 1947, 1949.

[redacted]

Figure 1.- Tunnel with side plate removed and cutaway outlet model mounted in upper floor.

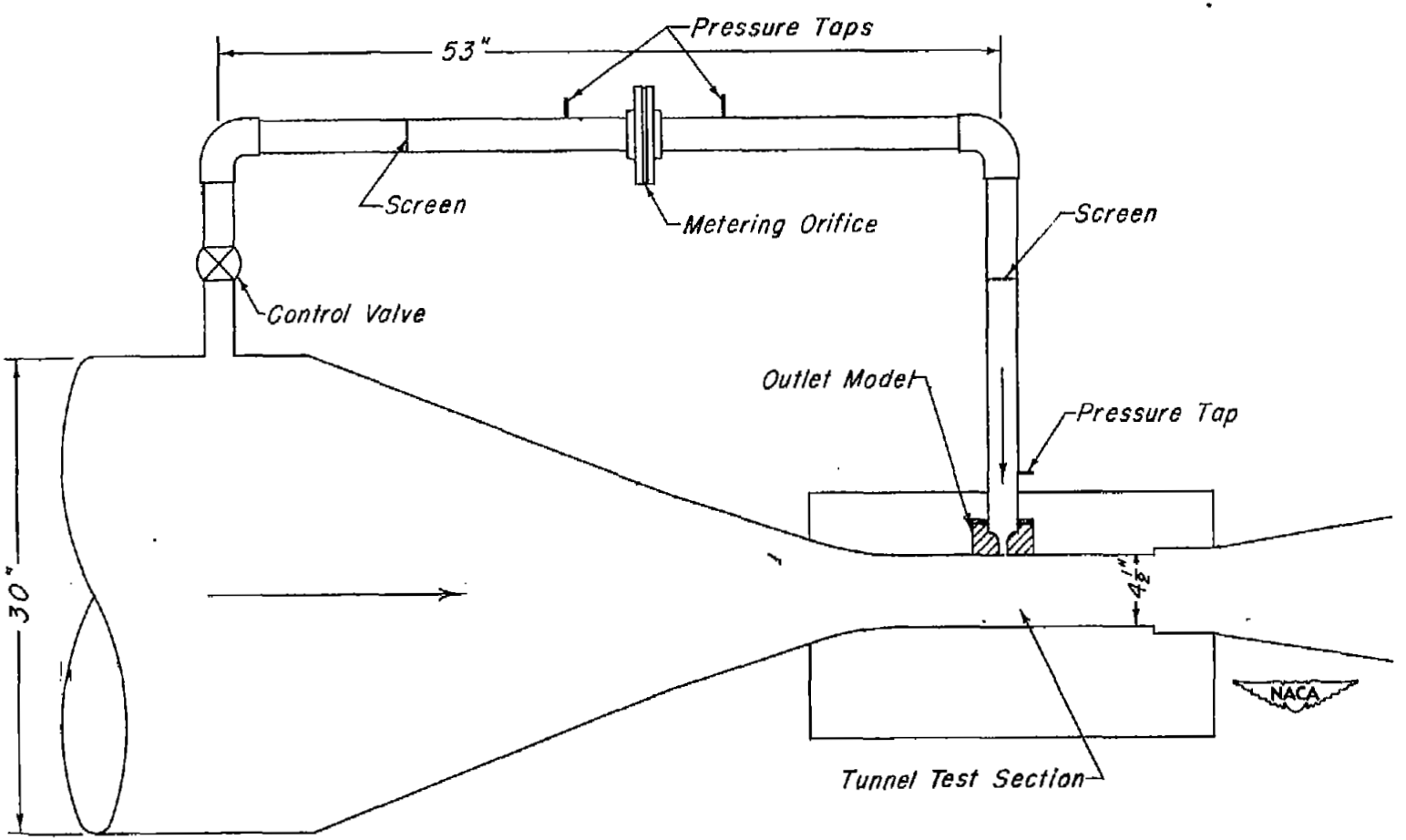

Figure 2.- General arrangement of tunnel and outlet air line.

Figure 3.- Outlet models.

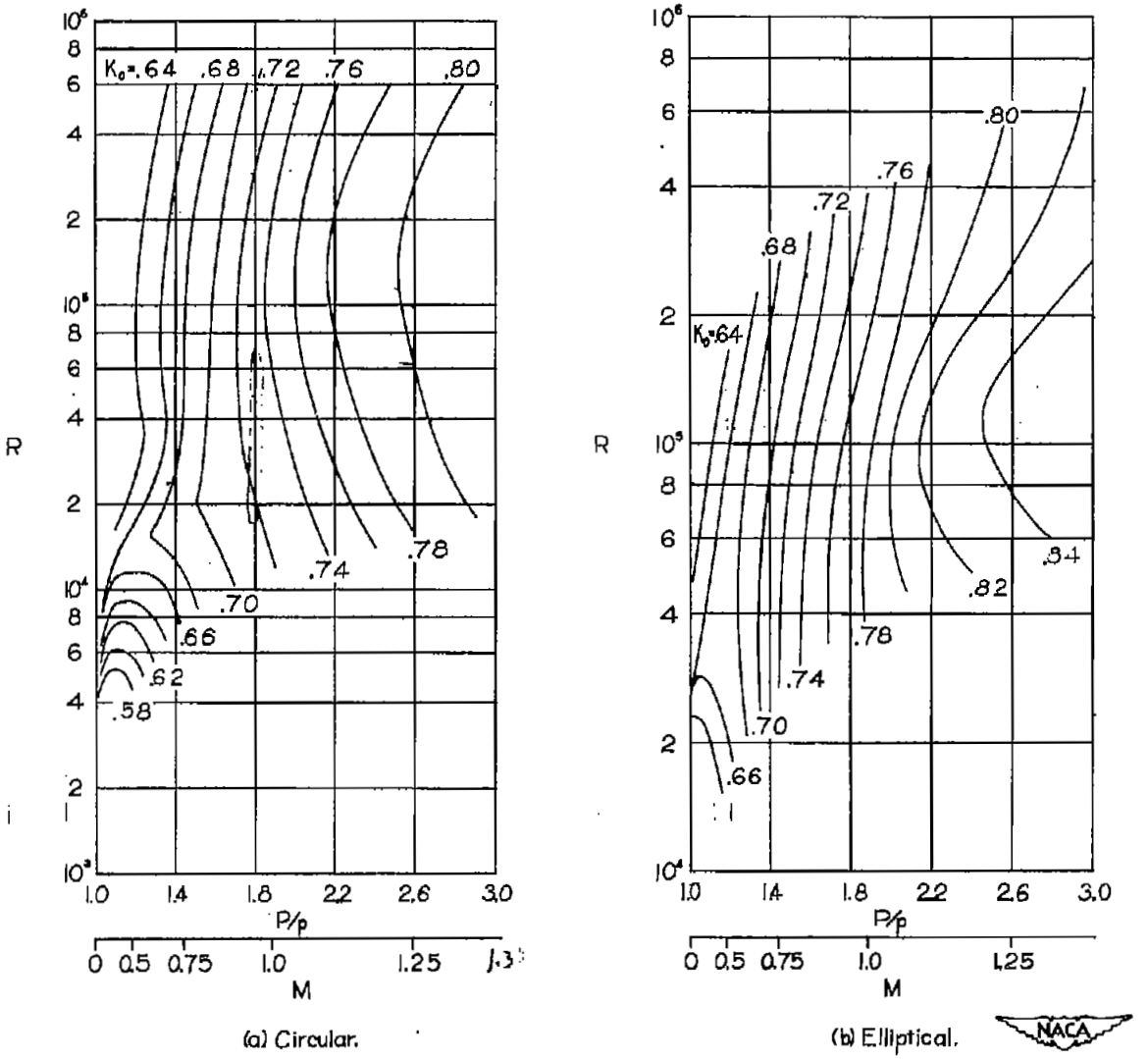

Figure 4.- Free-jet discharge coefficients for plate-type outlets.

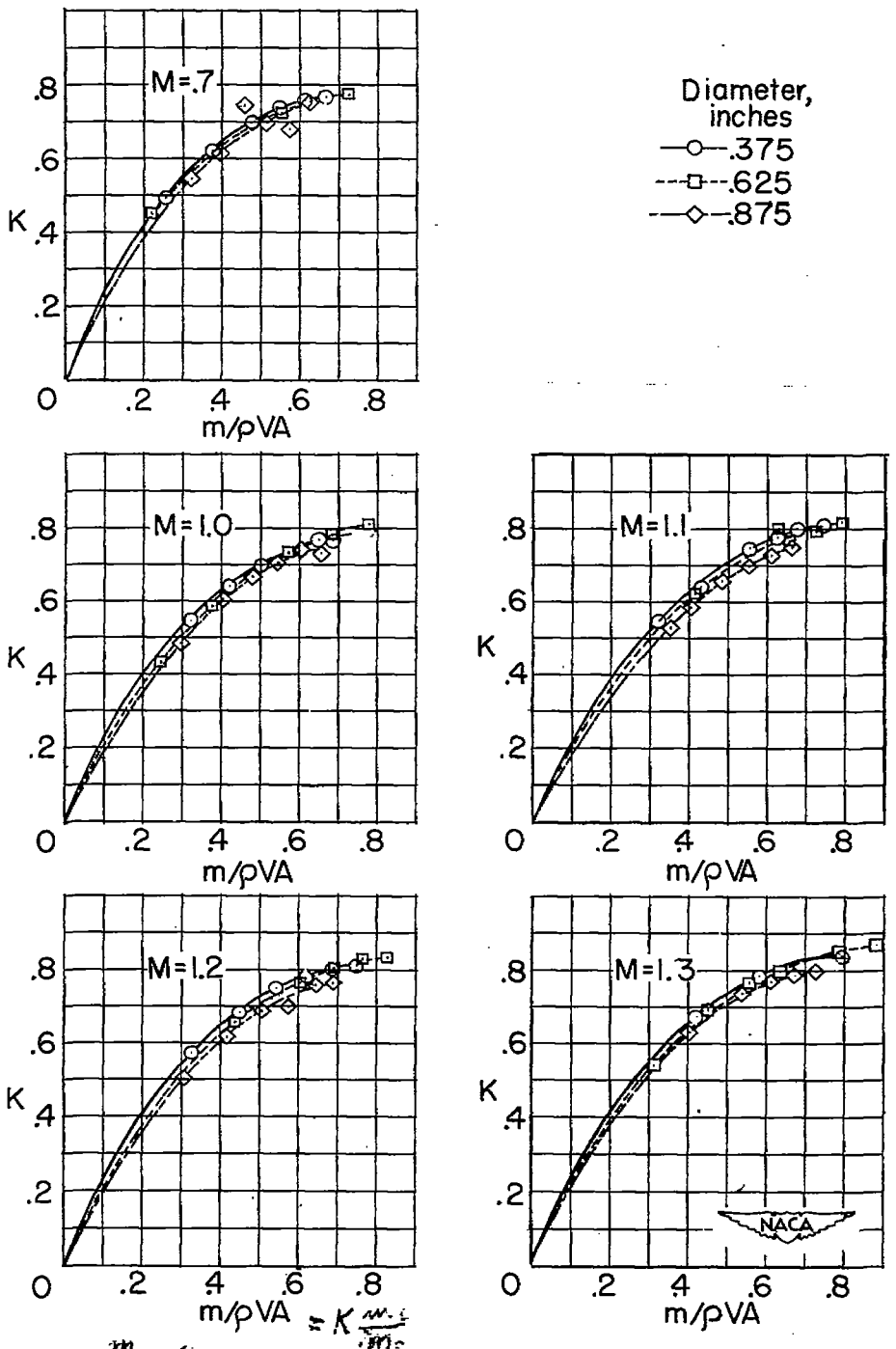

(a) Circular thin plate outlets.

Figure 5.- Outlet discharge coefficient as a function of flow rate and free-stream Mach number.

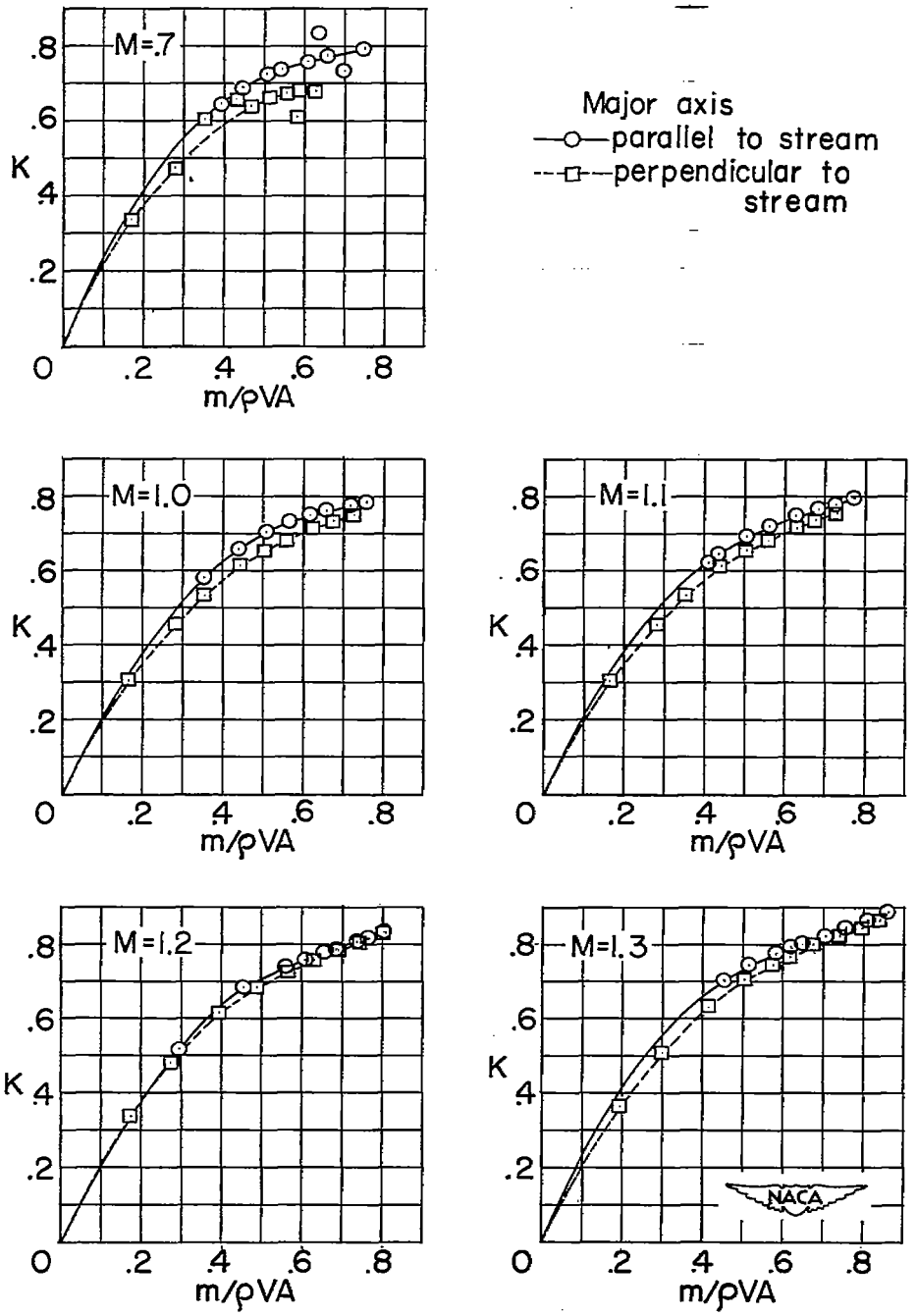

(b) Elliptical thin plate outlets.

Figure 5.- Continued.

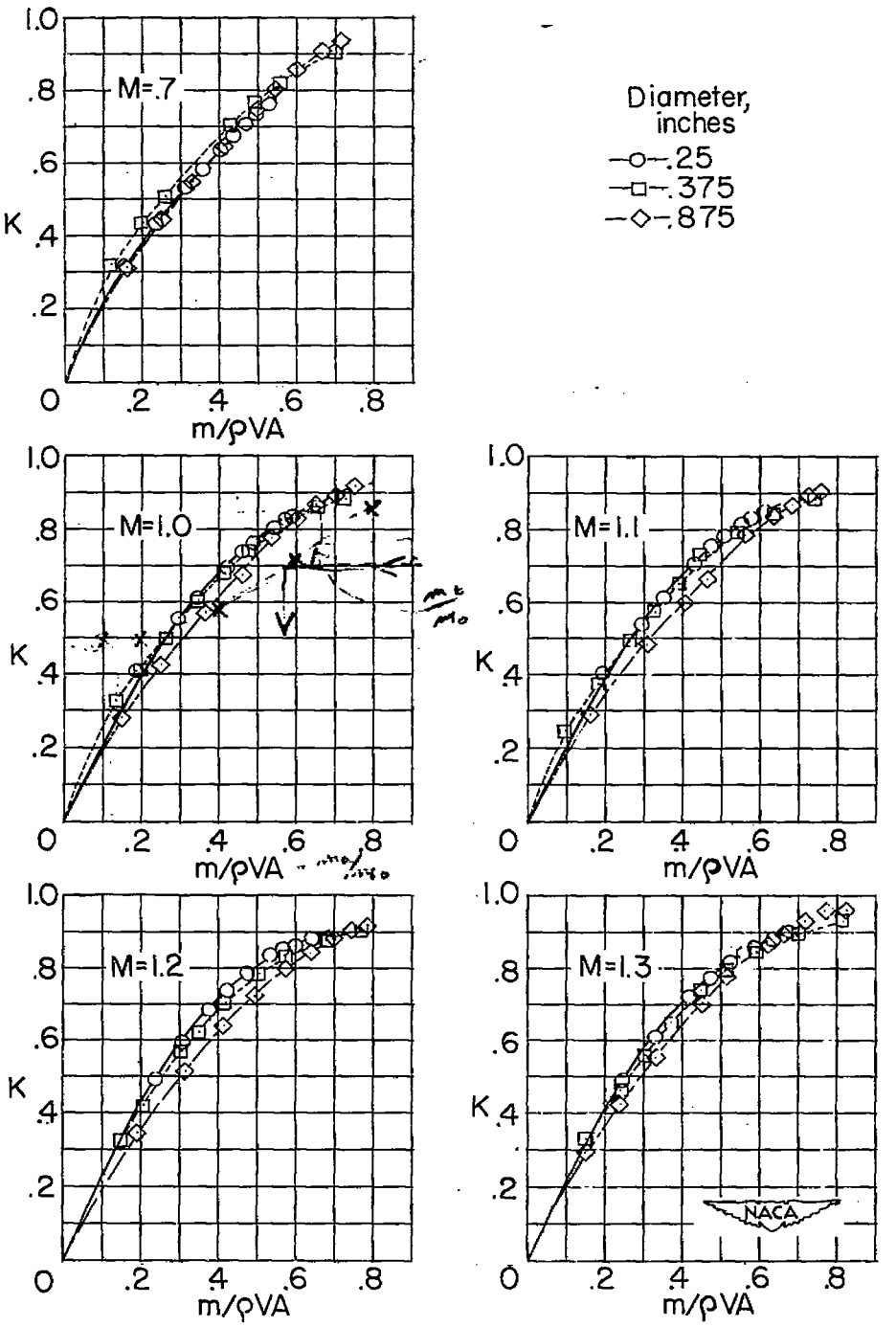

(c) Bellmouthed outlets.

Figure 5.- Concluded.

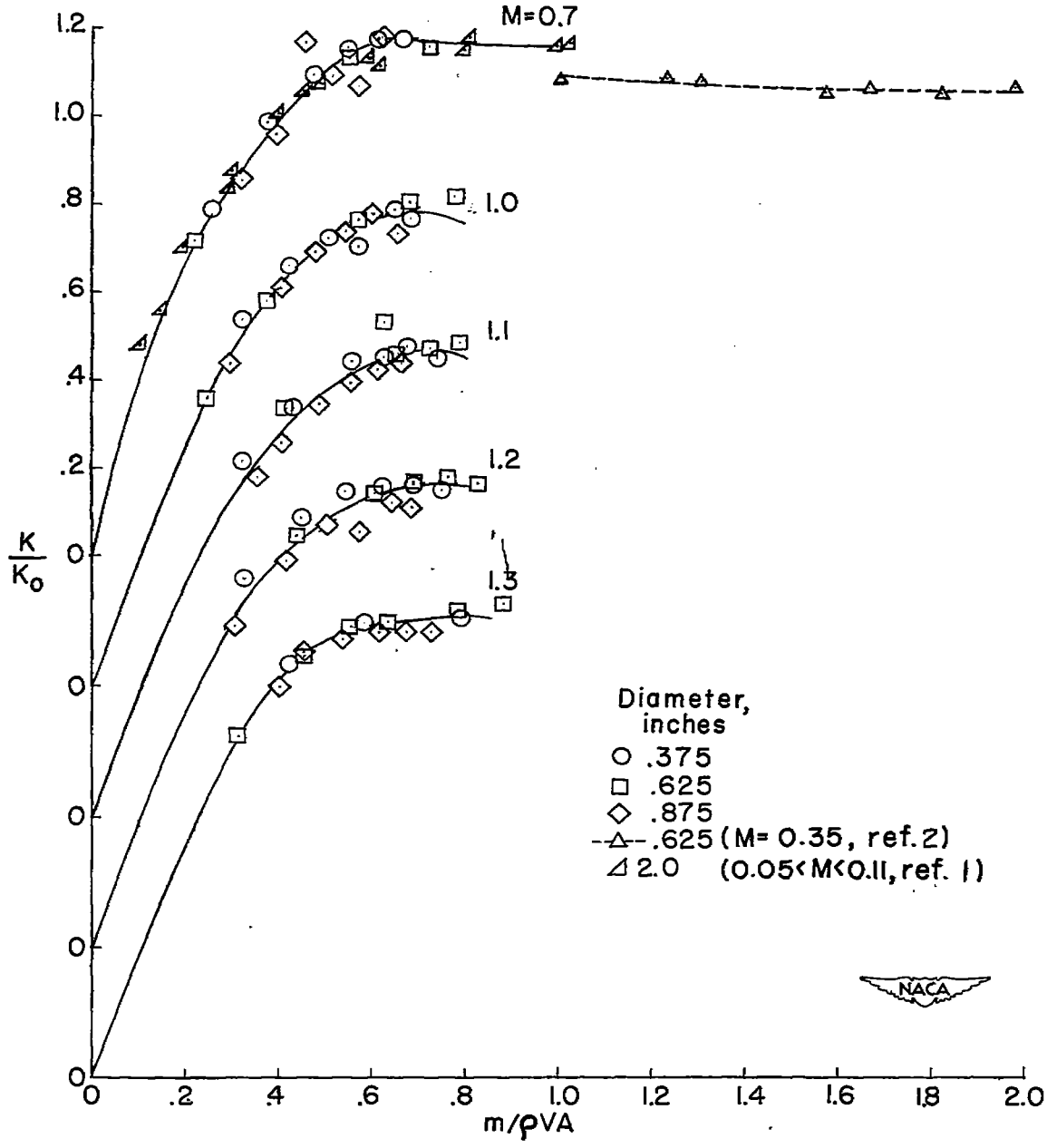

(a) Circular thin plate outlets.

Figure 6.- Outlet discharge coefficient relative to free-jet coefficient as a function of flow rate and free-stream Mach number.

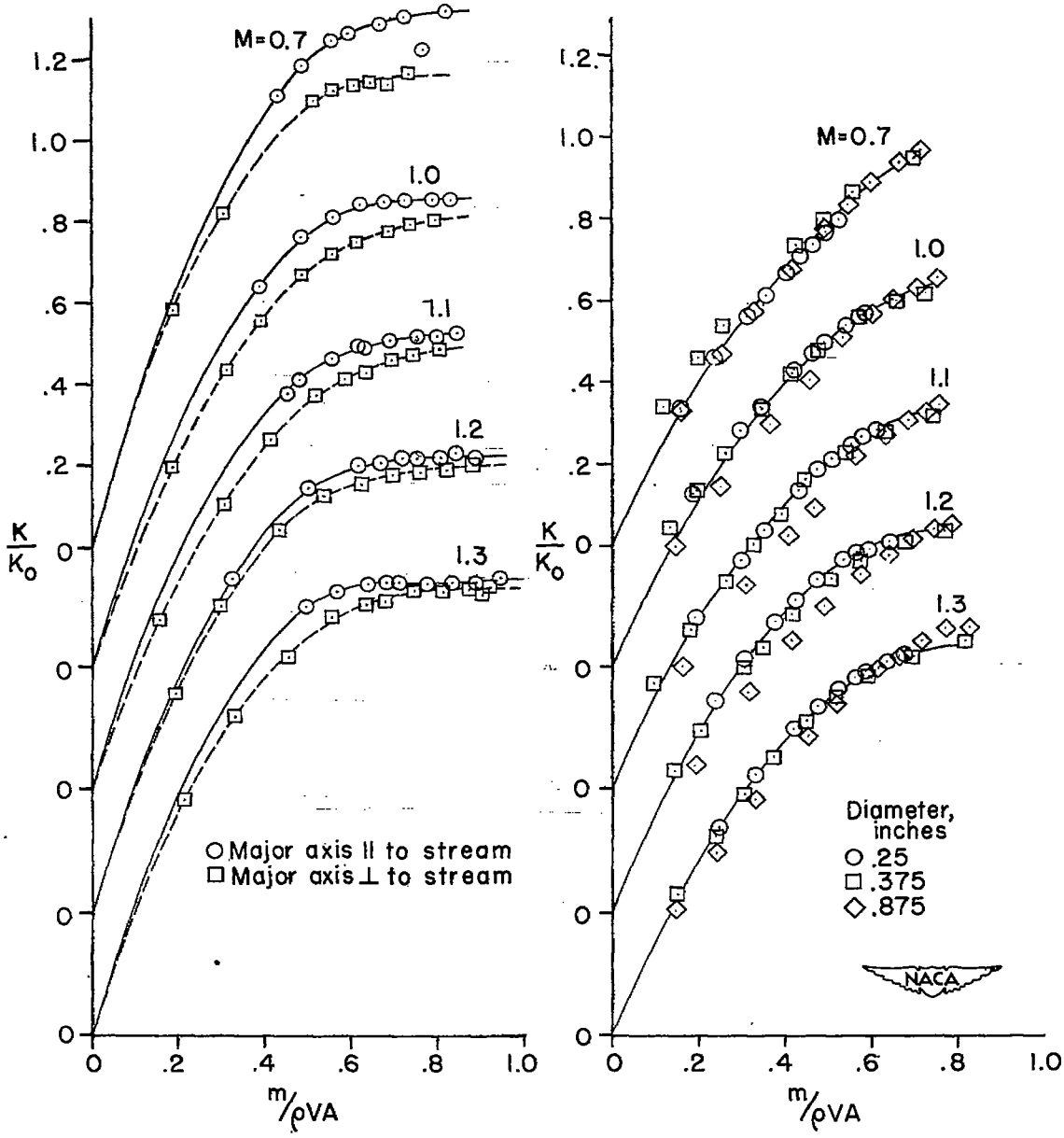

(b) Elliptical thin plate outlets.

(c) Bellmouthed outlets.

Figure 6.- Concluded.

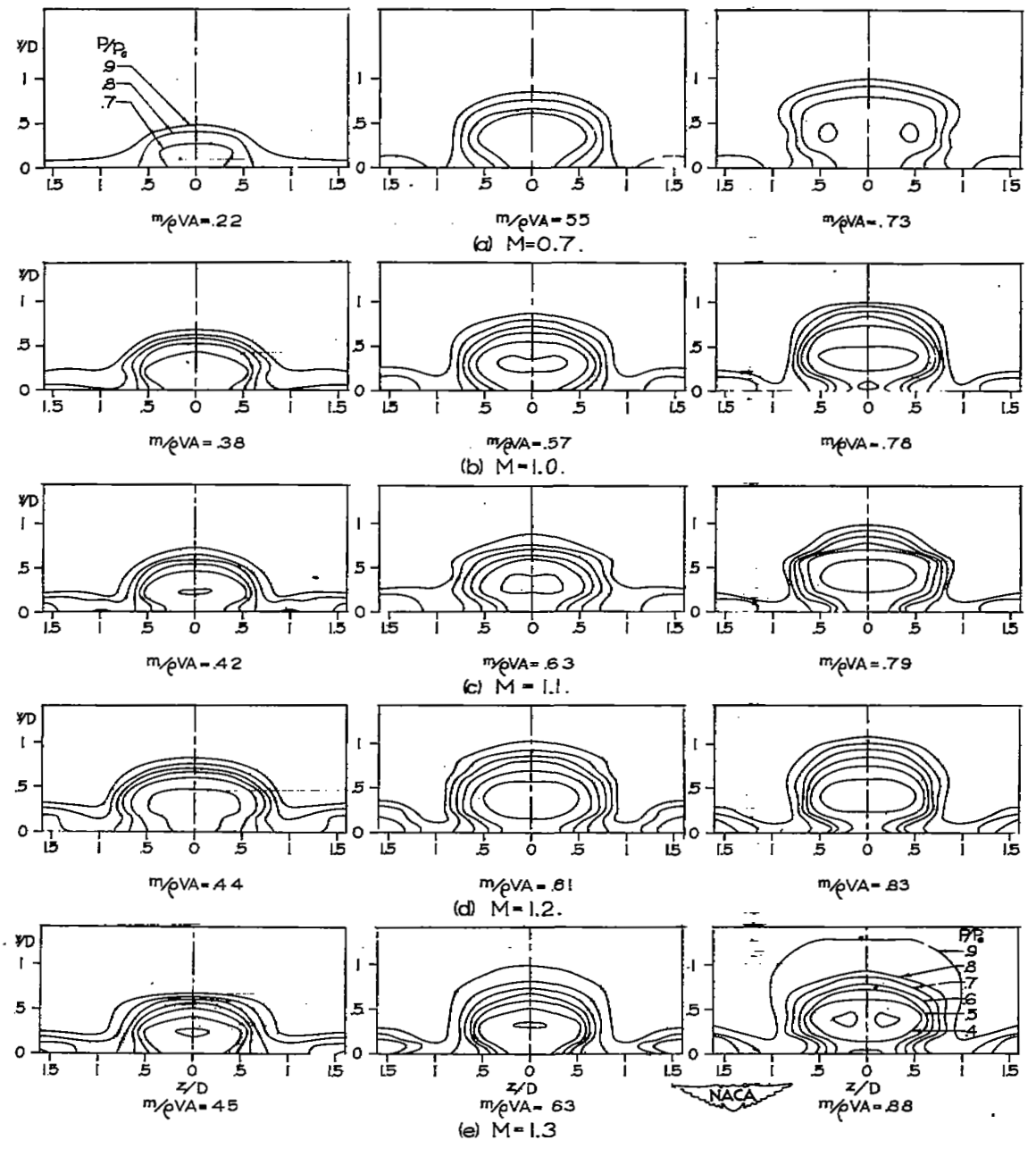

Figure 7.- Total-pressure distribution in wake of plate-type outlet at $\frac{x}{D} = 1.6$.

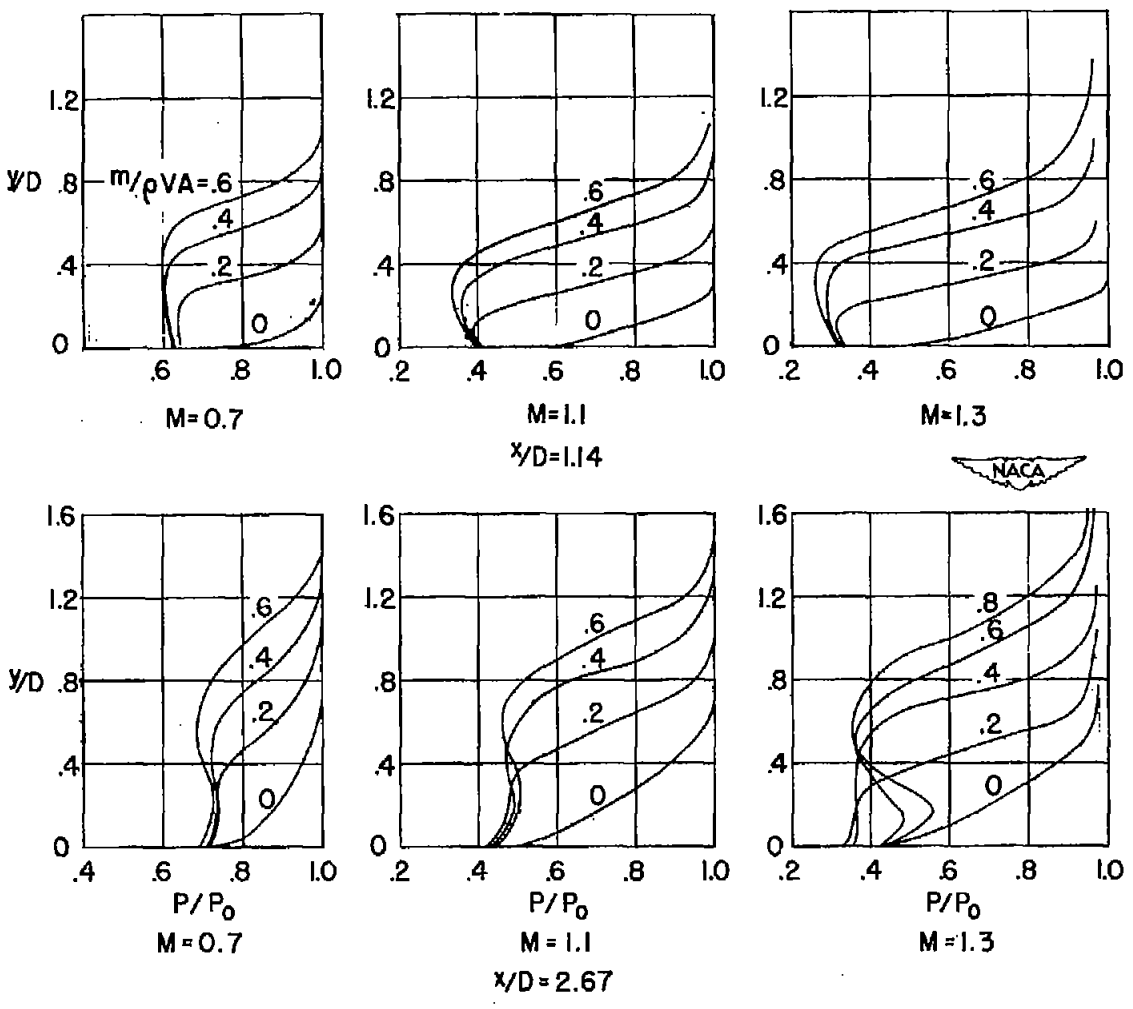

(a) Circular thin plate outlets.

Figure 8.- Total-pressure distribution through jet wake in plane of symmetry.

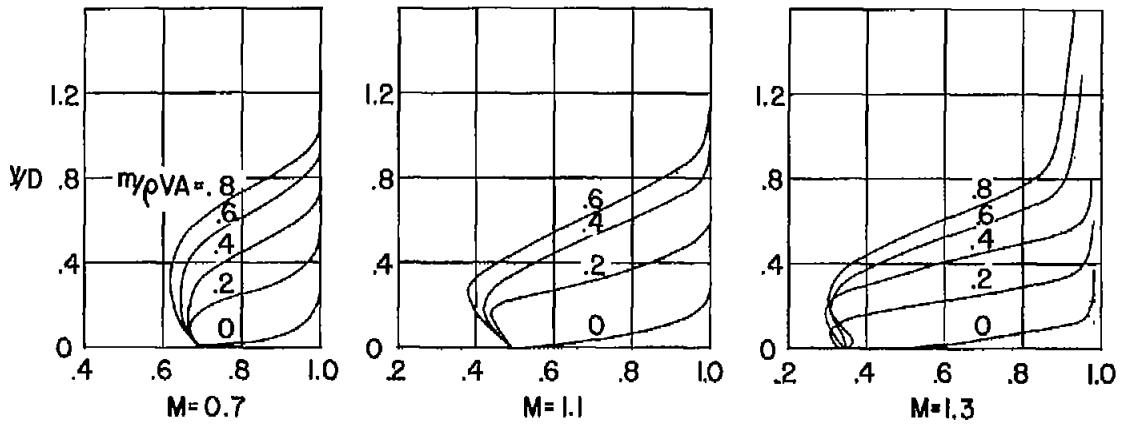

Major axis perpendicular to stream

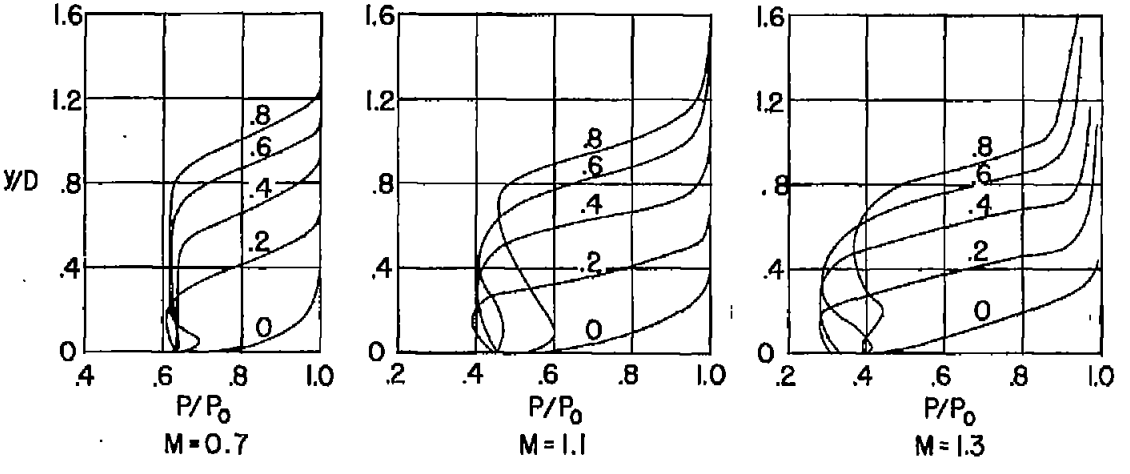

Major axis parallel to stream

(b) Elliptical thin plate outlets.

Figure 8.- Continued.

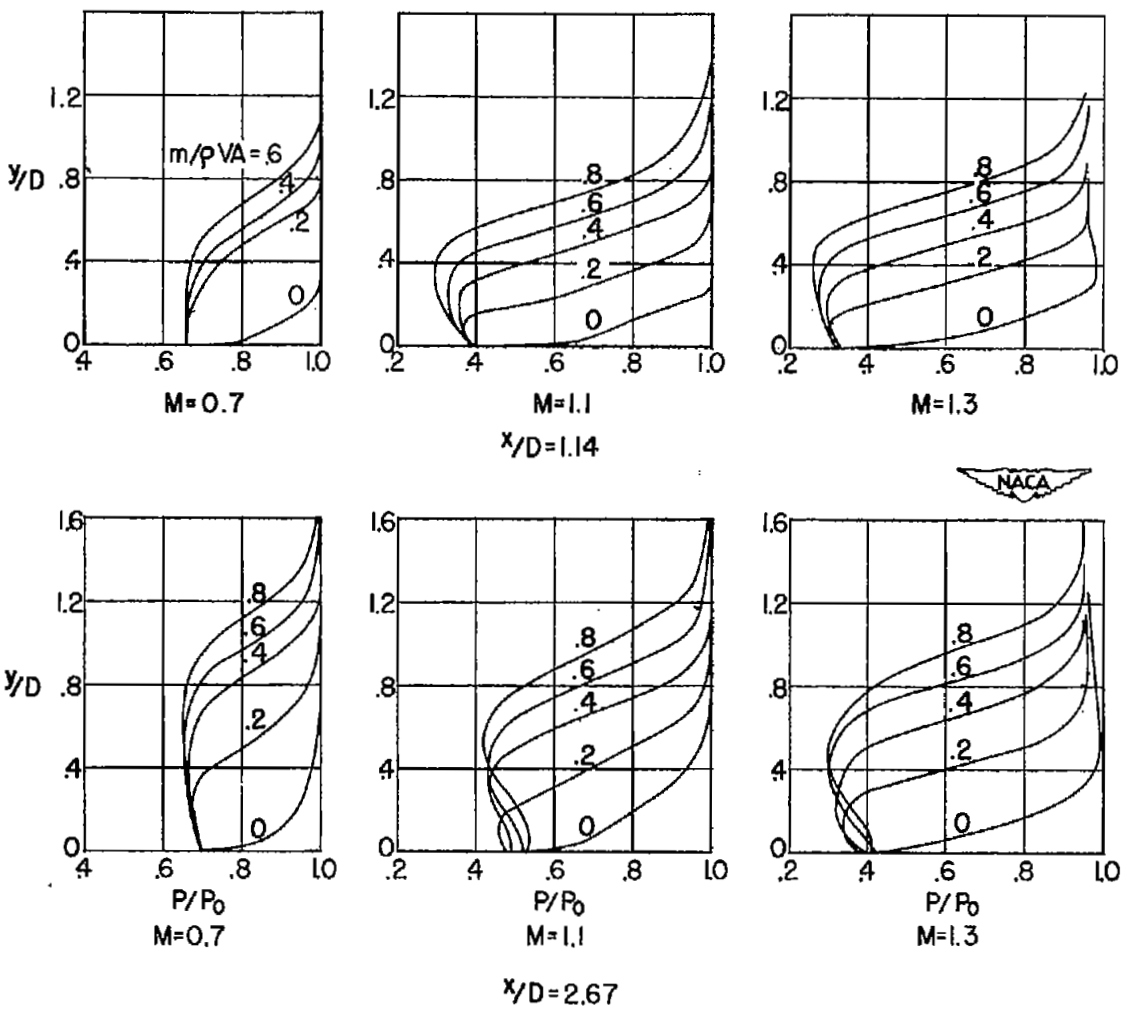

(c) Bellmouthed outlets.

Figure 8.- Concluded.

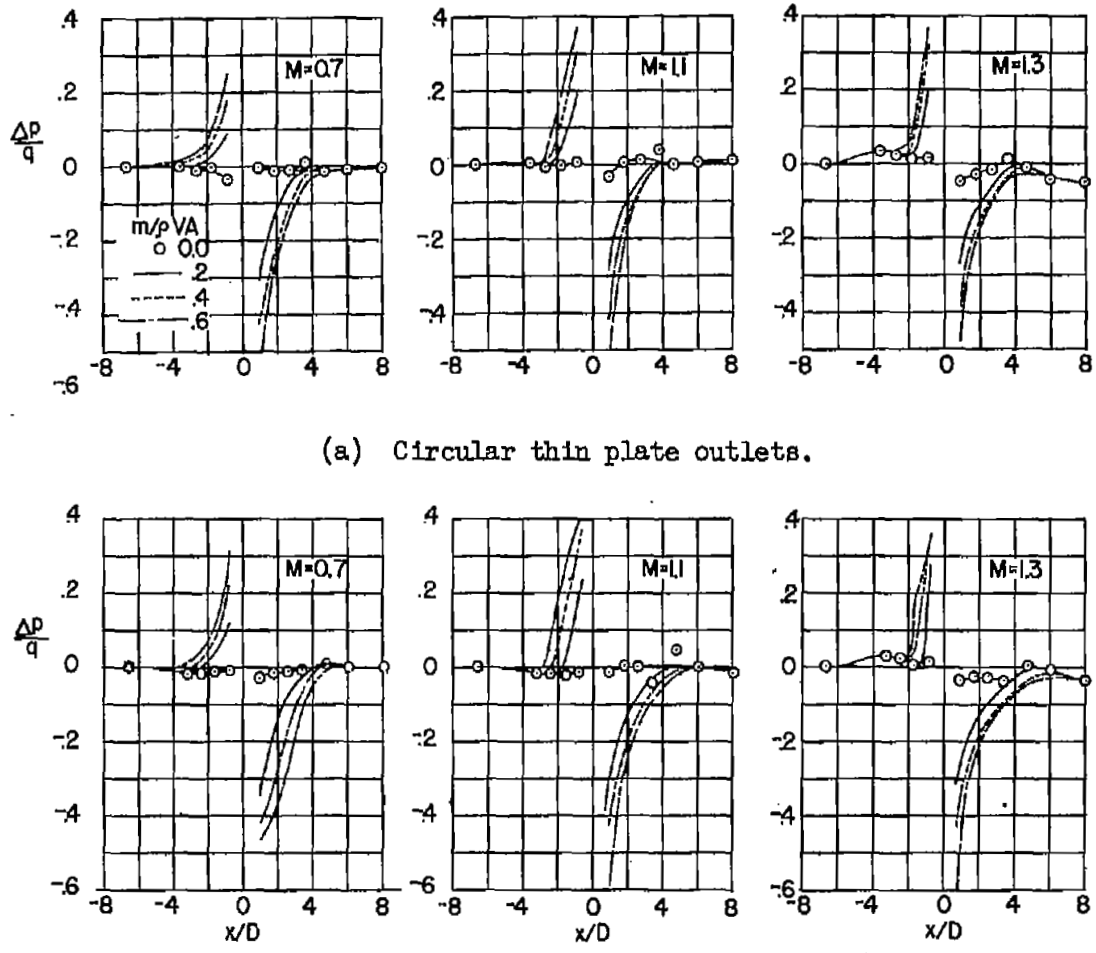

Figure 9.- Wall static pressure distribution along a line through the center of the outlet as a function of flow rate and free-stream Mach number.